# Voltage-controlled dissipation in the quantum Hall effect in a laterally constricted two-dimensional electron gas

J. R. Kirtley, Z. Schlesinger, T. N. Theis, F. P. Milliken, S. L. Wright, and L. F. Palmateer
*IBM Thomas J. Watson Research Center, P.O. Box 218, Yorktown Heights, New York 10598*
(Received 6 May 1986)

We have observed controlled, low-voltage breakdown of the quantum Hall effect in GaAs-$Al_xGa_{1-x}As$ heterostructures with lateral constrictions a few micrometers in width. The breakdown characteristics show structure at voltages corresponding to the cyclotron energy for even filling factors or the exchange-enhanced Zeeman energy for odd filling factors. Analysis of these results in terms of a simple model implies that the dissipation process involves interlevel as well as intralevel scattering, and therefore that large potential gradients must be present in the two-dimensional electron gas. We interpret structure at multiples of the cyclotron energy for even filling factors in terms of a multiple-current-path model.

## I. INTRODUCTION

When a two-dimensional electron gas (2D EG) is placed in a large perpendicular magnetic field at low temperatures, the density of states takes the form of discrete extended Landau levels separated by localized states.[1] If the electron density and magnetic field are such that the Fermi energy lies in the localized states between the Landau levels, the Hall resistance is precisely quantized.[2] This quantization occurs in part because scattering between states within a Landau level is forbidden by the Pauli exclusion principle, and dissipation is extremely small. However, when sufficiently large electric fields are applied to the 2D EG, dissipation occurs.[3-7] Ebert *et al.*[3] report a strong instability when electric fields of about 100 V/cm are applied in a magnetic field of 7 T. They attribute this breakdown to runaway of an electric-field-dependent electron temperature above a critical electric field. Cage *et al.*[4] report that the breakdown is spatially localized and that transient switching between distinct dissipative states occurs on a microsecond time scale.

In order for dissipation to occur, electrons must scatter parallel to the electric field. However, since this spatial translation involves a change in wave number, a source of momentum is required. It has been suggested that this momentum can be provided by scattering from impurities or by the emission of phonons.[8-11] There has been disagreement over whether breakdown in the quantum Hall effect involves scattering between states in the same Landau level (intralevel scattering)[8-10] or between different Landau levels (interlevel scattering).[11] Support for intralevel scattering comes from the fact that at the breakdown fields of 100 V/cm the drift velocity $v_d \equiv cE/B$, where $E$ is the Hall field and $B$ is the magnetic field, is near the speed of sound $v_s$. Above this critical drift velocity electrons can emit phonons and scatter to different states within the same Landau level while conserving energy and momentum. However, Heinonen *et al.*[11] argue that within the Born approximation, for an impurity-free system at integer filling factor, intralevel scattering cannot occur until states are emptied by interlevel scattering. They argue further that if the filling factor were somehow permitted to be below an integer value in order to allow intralevel scattering, then the predicted dependence of breakdown current on magnetic field would be incorrect.

On the other hand, interlevel scattering requires appreciable overlap between wave functions from different Landau levels. This happens if potential drops of order the cyclotron energy occur within a few cyclotron radii, requiring fields of order $10^4$ V/cm, much higher than the experimentally observed critical fields. It has been proposed that the local fields are much higher than the average fields due to spatial inhomogeneities, either near the edges, or within the bulk of the samples.

Previous experimental work has been done with samples so wide that breakdown occurred with total voltages across the samples of order volts, much larger than the characteristic energies in the system. We report here work in which the sample dimensions are small enough that breakdown occurs at voltages of order millivolts. In these samples the breakdown characteristics show structure at voltages corresponding to the cyclotron energies for even filling factors and the spin-enhanced Zeeman splittings for odd filling factors. A simple model is presented for these results which provides a natural explanation for the observation of structure at these energies, and for the roughly triangular dependence of breakdown field on filling factor. Analysis of the magnetic field dependence of the breakdown voltages in terms of this model indicates that both interlevel and intralevel scattering are involved in the dissipation mechanism. This implies that there are large spatial inhomogeneities in the potentials in these samples, since the average fields at breakdown are smaller than those required for interlevel scattering. Furthermore, under certain conditions structure in the breakdown characteristics is observed at multiples of the cyclotron energy. We interpret these results in terms of multiple current paths in the sample, and show that the data is consistent with the number of paths through the constriction changing as the Fermi level of the 2D EG is raised or lowered.

 ©1986 The American Physical Society

## II. EXPERIMENTAL DETAILS

It is very difficult to make narrow structures in GaAs heterojunctions that still yield high-quality data on Shubnikov–de Haas oscillations.[12] When the constriction is made too long and narrow, conduction is pinched off. We minimize this problem by making the constriction as short as possible. The geometry we use is shown in Fig. 1. In the Appendix we argue that our constriction geometry is equivalent to the more traditional Hall bar or Corbino geometries when the 2D EG is in the quantum Hall state. Our modulation-doped GaAs-$Al_xGa_{1-x}As$ heterojunctions are grown by molecular-beam epitaxy with a molar fraction $x=0.35$, a spacer layer 30 nm thick, and Si doping concentrations of $5\times10^{17}$ cm$^{-3}$. The 2D EG in our samples has electron mobilities of $(2-10)\times10^5$ cm$^2$/V s in the dark at 4.2 K, and electron densities in the range $(1.3-4)\times10^{11}$ cm$^{-2}$. The samples are photolithographically patterned and mesa etched through the $Al_xGa_{1-x}As$ layer and into the GaAs. The resulting mesas of $Al_xGa_{1-x}As$ are in the form of two overlapping squares a few millimeters on a side. Conduction between the squares occurs through a constriction a few micrometers wide. Contact is made to the 2D EG by alloying in 0.5-mm-diam balls of 98% In and 2% Sn. Two contacting geometries are used. In the pseudo-Hall bar geometry, contacts are made to the edges of the 2D EG [Fig. 1(c)], current is run between contacts 1 and 2, the longitudinal resistance is determined from the voltage drop between contacts 3 and 4, and the Hall voltage is measured between contacts 3 and 5. In the pseudo-Corbino geometry contacts are made internal to the 2D EG [Fig. 1(d)], and two terminal measurements of the conductance are made.

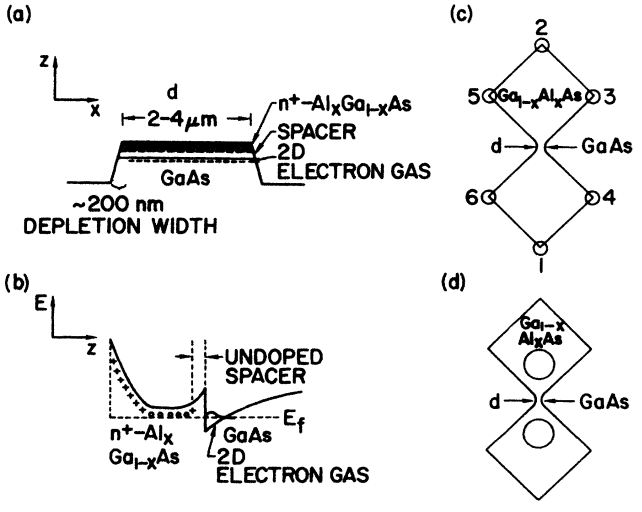


FIG. 1. Sample geometry of our GaAs-$Al_xGa_{1-x}As$ heterojunction constrictions: (a) Cross section through the waist of the butterfly-shaped mesa. (b) Energy-level diagram of the conduction-band discontinuity and 2D EG trapped at the interface between the $Al_xGa_{1-x}As$ and the GaAs. (c) Contact geometry for the pseudo-Hall bar samples. (d) Contact geometry for the pseudo-Corbino geometry samples.

After fabrication, the samples are mounted on headers, cooled slowly in the dark, and a magnetic field is applied perpendicular to the heterojunction interface. The dynamic resistance or conductance is measured using standard modulation techniques. Identical results are obtained when the modulation frequencies are varied from 11 Hz to 1.1 kHz, or by numerically differentiating current-voltage characteristics.

## III. RESULTS

All of the samples studied show the same qualitative behavior. For the pseudo-Hall bar geometry samples, when the magnetic field is adjusted to a resistance minimum, there is an onset in resistance when the current through the constriction increases above a critical value. This critical current is related to a critical Hall voltage through the Hall resistance. Similarly, for the pseudo-Corbino samples, there is an onset in conductance when the voltage across the constriction increases above a critical value. Although the changes in slope in the breakdown characteristics tend to be fairly sharp, the definition of the critical voltage above which dissipation begins is somewhat arbitrary in the absence of a detailed theory for the onset of dissipation. We obtain very similar results for the critical voltage if we linearly extrapolate the breakdown characteristics to zero dissipation, or if we define the critical voltage to be that required to make the resistance (conductance) exceed a given small value. In either case the critical voltage is largest near the center of the magnetoresistance (magnetoconductance) minimum and has a roughly triangular dependence on field away from that point. Although all samples studied in the pseudo-Hall bar geometry show low voltage ($eV_h<100$ mV) breakdown, only those below about 6 $\mu$m in width show sharp structure at voltages corresponding to the gap energies. Samples below about 3 $\mu$m in width tend to be "pinched off;" i.e., they do not show high-quality oscillations in the magnetoresistance until their electron concentration is raised by exposure to light. After exposure to light these samples show structure in the breakdown characteristics at the gap energies, but the characteristics are highly asymmetric, indicating that large built-in potentials exist in the constriction region. Samples wider than about 6 $\mu$m lack the sharp structures observed with the narrower samples and do not show appreciable dissipation until voltages larger than the gap energies are applied. In the pseudo-Hall bar samples we demonstrate the breakdown to be in the constriction region by monitoring the multiple contacts.

We also observe structure at the gap voltages in the breakdown characteristics in five of the nine pseudo-Corbino samples studied. The samples which show these effects have In contacts close (within a few tenths of a millimeter) to the mesa edge. Furthermore, in two of the samples, structure at the gap energies is observed even when current is passed between two contacts internal to but close to the edge of the same pad. We hypothesize that spatial inhomogeneities, as well as narrow constrictions, can create the conditions necessary for low-voltage breakdown to occur. The insets of Fig. 2 show the con-

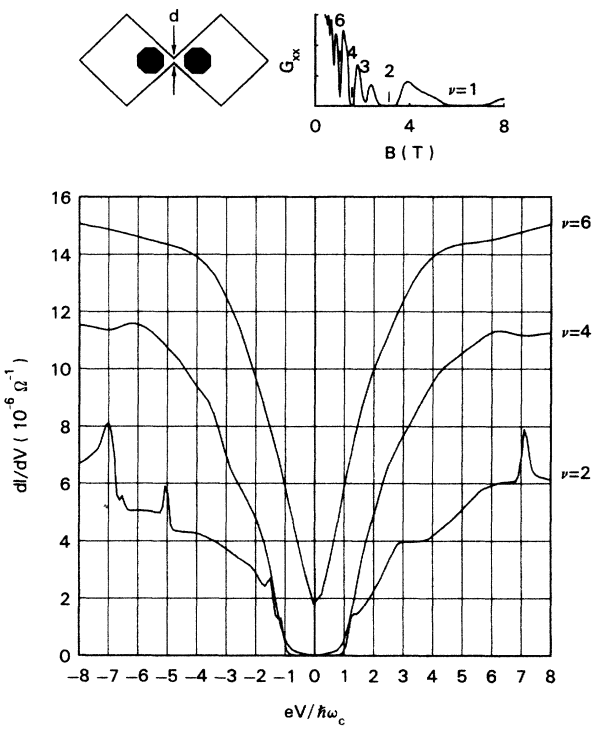


FIG. 2. The left inset shows the pseudo-Corbino contact geometry. The right inset shows Shubnikov—de Haas oscillations in the conductance with perpendicular magnetic field for the pseudo-Corbino geometry No. 1 (also known as V-69). This sample has a constriction width of about 4 $\mu$m. The main figure shows the dynamic conductance versus reduced voltage $eV_c/\hbar\omega_c$ breakdown characteristics for this sample for fields of 3.23, 1.55, and 1.06 T, corresponding to the centers of the magnetoconductance minima for filling factors 2, 4, and 6, respectively. The temperature is 0.3 K, the modulation voltage is 35 $\mu$V rms at 100 Hz.

tacting geometry and the oscillations in conductance with magnetic field for the pseudo-Corbino sample No. 1 (also known as V-69), at 0.3 K. The main figure shows the dynamic conductance versus reduced voltage $eV/\hbar\omega_c$ for fields at the center of the magnetoconductance minima, (as marked in the magnetoconductance inset), for even filling factors 2, 4, and 6. Here $\hbar\omega_c$ is the cyclotron energy, set equal to $1.7B$, where $\hbar\omega_c$ is measured in meV, and the magnetic induction $B$ is in teslas. For filling factor $\nu=2$ there is a break in the slope of the conductance versus voltage characteristic at a critical voltage set by the cyclotron energy. Above this voltage the conductance increases until it is comparable to the conductance of the sample outside of the magnetoconductance minima. Further, there is additional structure at multiples of the cyclotron energy. Unlike the structure in the breakdown characteristics at the cyclotron energy, these peaks are not reproducible in amplitude from cooldown to cooldown. The breakdown characteristics are also asymmetric in voltage. For example, in Fig. 2 there is a strong peak at $eV=5\hbar\omega_c$ for negative biases but not one for positive biases. This asymmetry reverses itself, in the sense that structure at negative bias appears at positive bias, when the direction of the magnetic field is reversed. In Fig. 2 the structure appears primarily at odd multiples of the cyclotron energy; as we will see below, sometimes the structure also appears at even multiples. The change in slope of the breakdown characteristic for the $\nu=4$ filling factor is more rounded, but occurs at much the same voltage as for the $\nu=2$, when normalized by the concentration energy. When the magnetic field is reduced further to the $\nu=6$ filling factor, the conductance never "bottoms out," and the breakdown characteristic at the magnetoconductance minimum does not show an onset in conductance above a critical voltage.

For both contact geometries low-voltage breakdown of the quantum Hall state occurs for odd, as well as even, filling factors. Figure 3 shows the breakdown characteristics for the $\nu=3$ filling factor for the pseudo-Corbino geometry sample No. 1 for a number of different temperatures. Previous work on breakdown of the dissipationless quantum Hall state using wide samples[3] showed that the critical field was temperature dependent. This is not the case for the data of Fig. 3. The observed gap in conductance becomes smeared in voltage as the temperature increases, and there is an additional background conductance, but the position of the structure, as measured, for example, by the peak in the derivative of the conductance, does not move appreciably as the temperature increases. Were the relation $V_c=\Delta/e$ (where $\Delta$ is the energy gap) to hold for spin-split levels, the peak value of 0.3 mV for the

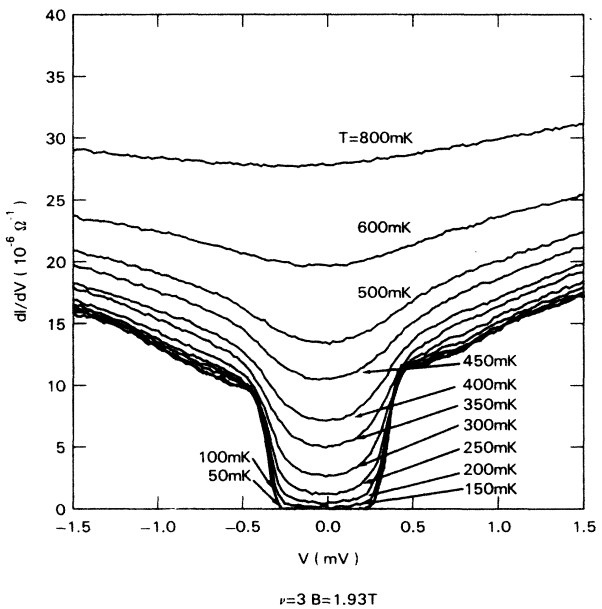


FIG. 3. Temperature dependence of the breakdown characteristics for the pseudo-Corbino sample No. 1 for $\nu=3$ filling factor at a field of 1.93 T. The modulation voltage is 5 $\mu$V rms at 100 Hz. The low-temperature critical voltage for the onset of conductance is about 0.3 meV. This corresponds to an exchange enhanced $g$ factor of about 2.7 for this filling factor.

$\nu=3$ level would correspond to an exchange-enhanced Zeeman splitting $g$ factor of $g^*=eV_c/\mu_B H=2.7$, where $\mu_B$ is the Bohr magneton. This value is in reasonable agreement with that obtained by Englert *et al.*[13] ($g^*=2.6$ at $T=1.4$ K) for the $\nu=3$ level from measurements of the temperature dependence of the magnetoresistance of a wide 2D EG sample. The activation energy for this state, as measured by fitting the low-temperature conductance at zero bias to the expression $\sigma_{xx}\sim e^{-E_a/k_BT}$, is 0.2 eV, lower than that obtained from the breakdown characteristic. We speculate that this difference could be the result of the finite level width of the spin-split levels.

Previous workers on breakdown of the quantum Hall effect in wide samples have noted a roughly triangular dependence of the critical breakdown fields on applied magnetic field.[3] This is also true for our narrow samples. Figure 4 shows the dependence of the breakdown characteristics for the pseudo-Corbino sample No. 1 for magnetic fields around a filling factor of 3 at $T=40$ mK. As the magnetic field is reduced from 2.064 T, increasing the filling factor, the gap in conductance increases in width until it reaches a maximum of 0.3 meV at 1.955 T. As the filling factor is increased further, the gap decreases again.

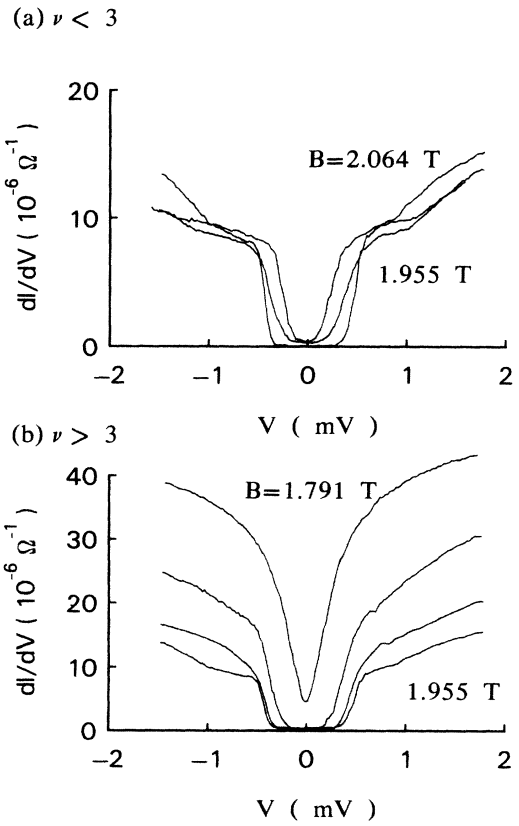


FIG. 4. Magnetic field dependence of the breakdown characteristics for the pseudo-Corbino sample No. 1 near the $\nu=3$ filling factor at a temperature of 17 mK. The modulation voltage is 5 $\mu$V rms at a frequency of 100 Hz. Successive curves are evenly spaced in magnetic field.

The roughly triangular dependence of the critical voltage for the onset of dissipation on magnetic field is also observed for filling factors that are near even integers. The insert in Fig. 5 shows the Shubnikov–de Haas oscillations in resistance for the pseudo-Hall bar sample No. 2 (also known as V-125x) at 0.33 K. Measurements of the Hall voltage at low currents show plateaus in resistance equal (to within our measurement accuracy of $\mp 1\%$) to the accepted values for the quantized Hall resistance.[14] Figure 5(a) shows the resistance across the constriction versus reduced Hall voltage $eV_h/\hbar\omega_c$ for sample No. 2 with fields around $\nu=6$. Here $V_h=IR_h=Ih/ve^2$ is the Hall voltage, and $R_h$ is the quantized Hall resistance. As the field is reduced from 2.5 T, the third Landau level is filled and the longitudinal resistance at low currents (and

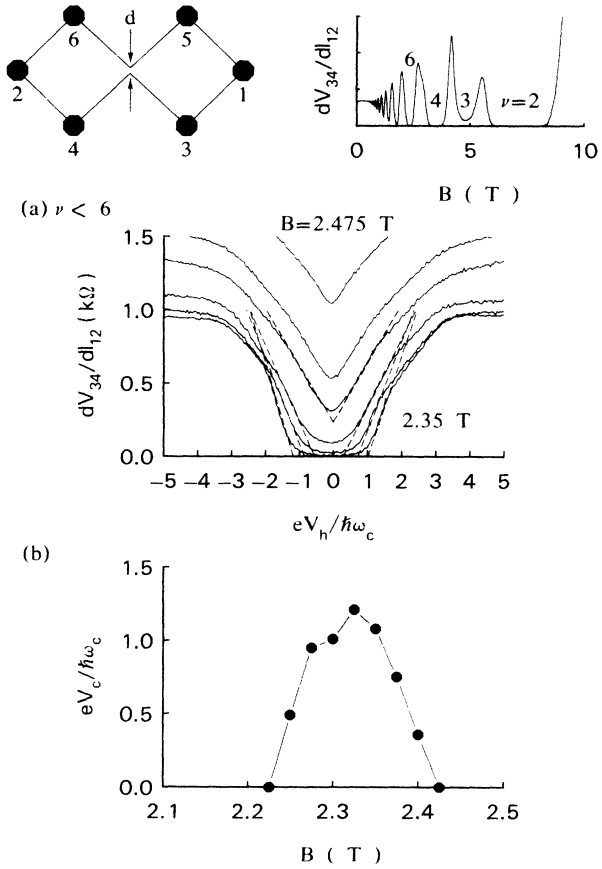


FIG. 5. Magnetic field dependence of the breakdown characteristics for the pseudo-Hall bar sample No. 2 (also known as V-125x) ($d=4$ $\mu$m) near the $\nu=6$ filling factor. The upper-left inset shows the contact geometry for this sample, the right inset shows Shubnikov–de Haas oscillations in the longitudinal resistance $R_{xx}$ at zero bias current for this sample. Each successive curve in (a) is spaced by 0.025 T from the last. The measurements are taken at 1.4 K with a 10-nA rms modulation current at 10 Hz. The dashed lines in (a) are a linear extrapolation of the data to the horizontal axis. The reduced critical Hall voltages $eV_c/\hbar\omega_c$, taken to be the average of the absolute values of the intercepts of these lines for the two opposite bias polarities, are shown as a function of magnetic field in (b).

therefore low Hall voltages) decreases. At the same time a critical current for a change in slope of the resistance versus Hall characteristics develops. The dashed lines in Fig. 5(a) extrapolate the resistance versus Hall voltage data to zero resistance to obtain a critical Hall voltage. In Fig. 5(b) we plot the reduced critical Hall voltages $eV_c/\hbar\omega_c$, defined in this way, versus magnetic field for this sample. This critical Hall voltage is largest at the field where the zero bias resistance is smallest; i.e., when the Fermi energy is midway between the Landau levels. At this field the critical Hall voltage is roughly equal to the cyclotron energy. As the field is decreased further to the point where the next higher Landau level begins to be filled, the resistance at zero bias increase again and the critical Hall voltage decreases.

We show in Fig. 6 the breakdown characteristics for the same sample as in Fig. 5 at fields around a filling factor of $\nu=2$. In Fig. 7 we show the reduced critical Hall voltages for onset of dissipation for this sample as a function of inverse magnetic field. The critical Hall voltages are defined to be those voltages at which the sample has a dynamic longitudinal resistance of 100 Ω, about 1% of the dynamic resistance between magnetoconductance minima. Also plotted in Fig. 7 are the reduced thermal activation energies for this sample as a function of field. As the field is decreased from 8 T, increasing the filling factor and raising the Fermi level, the critical voltages increase. For low filling factors the critical voltages are about 2 meV larger than the activation energy. However, when the field is reduced below 7.4 T, the critical-voltage curve breaks away from the activation-energy curve until the critical voltage is about $4\hbar\omega_c/e$. As the field is re-

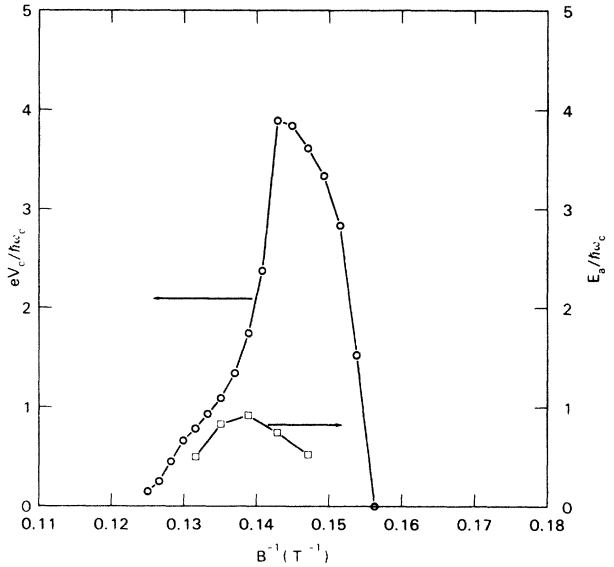


FIG. 7. Reduced critical Hall voltage $eV_c/\hbar\omega_c$ (as defined in the text) versus inverse magnetic inductance $B^{-1}$ for the data. Also shown for comparison is the magnetic field dependence of the activation energies for this sample. At low filling factors the critical voltages follow the activation energies, aside from a 2-meV shift possibly due to a finite level width. We interpret the divergence between the two curves at high filling factors as due to opening of multiple conduction channels.

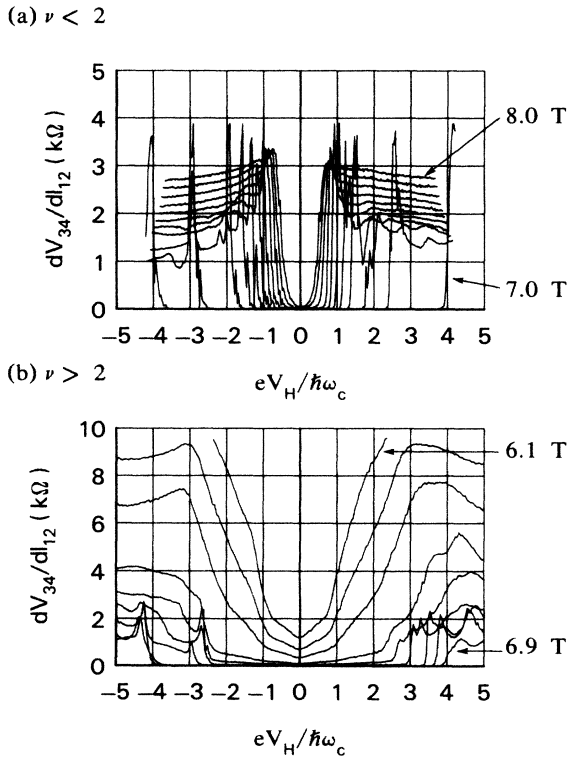


FIG. 6. Magnetic field dependence of the breakdown characteristics for the pseudo-Hall bar sample No. 2 near a filling factor of $\nu=2$. The temperature is 0.35 K, and the modulation current is 10 nA rms at 10 Hz. Each successive curve is spaced by 0.1.

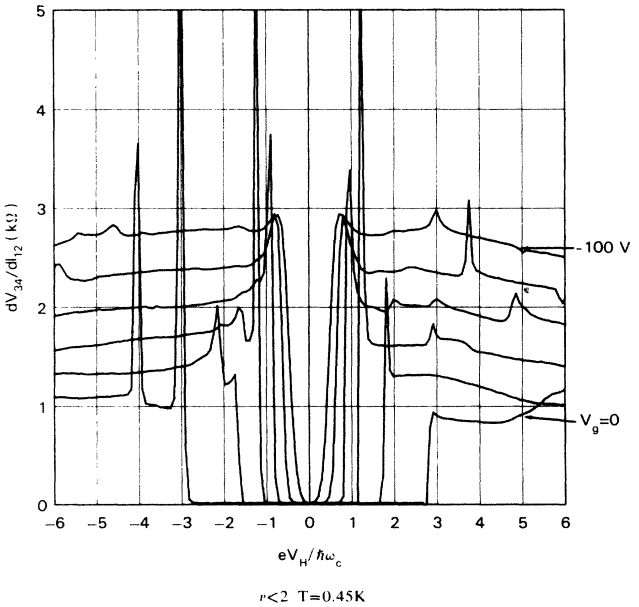


FIG. 8. Gate-voltage dependence of the breakdown characteristics for the pseudo-Hall bar sample No. 2. The temperature is held at 0.45 K, the field at 7 T, with a modulation current of 10 nA rms at 10 Hz. Each successive curve is spaced in gate voltage by 20 V.

duced further, the critical voltages decrease, but residual structure at around $\hbar\omega_c$ becomes visible again when the field falls below about 6.2 T.

Very similar results are obtained by changing the electron density with a back gate at constant field as are obtained by changing the magnetic field at constant electron density. Figure 8 shows the breakdown characteristics for the pseudo-Hall bar geometry sample No. 2 at $T=0.45$ K, a field of 7 T, for gating voltages every 20 V from 0 to $-100$ V. Shubnikov–de Haas measurements of the electron densities for this sample give $3.24\times10^{11}$ cm$^{-2}$ for no gate voltage, $2.93\times10^{11}$ cm$^{-2}$ for $-100$ V, and $3.58\times10^{11}$ for $+100$ V gate voltage. Just as when the Fermi energy is moved by changing the magnetic field (see Fig. 6), the gap increases to about a value of $\hbar\omega_c$ as the filling factor is increased, and then rapidly becomes large. The sharp structures near multiples of the cyclotron energy are also very striking in this data, and occur at even as well as odd multiples of the cyclotron energy.

## IV. DISCUSSION

### A. Single-channel picture

Several theoretical studies of the distribution of current in a Hall-bar sample in the quantum Hall state indicate that the current should flow within a few cyclotron radii of the edges.[15–17] However, experimental studies show that the current flows through the bulk of the sample and can be highly inhomogeneous.[18] We assume that the spatial inhomogeneity in current flow is due to multiple current paths flowing through wide samples. Our samples which show structure in the breakdown characteristics at the cyclotron energies are not much wider than samples which show no high-quality Shubnikov–de Haas oscillations. We interpet this to mean that they are nearly narrow enough to be pinched off. We assume in the analysis below that under certain conditions of electron density and magnetic field these samples have only one continuous conducting channel through the constriction. Further, we assume that the current is carried through this channel at its edges.

We show that given these assumptions an onset of dissipation can be expected for voltages above the cyclotron energy. For dissipation to occur, filled electronic states must scatter parallel to the electric field into previously empty states (see Fig. 9). We wish to calculate the effective electrochemical potential for the current-carrying states of a single channel as a function of filling factor, current, and position across the channel. If there are filled states as high in energy as some portion of the next higher unoccupied Landau level, then interband scattering to that level is energetically allowed and dissipation can occur if the local potential gradients are large enough. If there are empty states as low or lower than the energy of some section of the same Landau level, then intraband scattering is energetically allowed and can occur if, for example, the current density is high enough for scattering by phonon emission to occur.

We calculate the electrochemical potential following a procedure of Heinonen and Taylor.[15] The solution to Schrödinger's equation for a 2D EG in a magnetic field $\mathbf{B}=B\hat{\mathbf{z}}$ in a potential $V=V(x)$ takes the form of plane waves with wave vector $k$ in the $y$ direction and solutions to the one-dimensional harmonic-oscillator equation in the $x$ direction. The wave functions are labeled by the Landau-level quantum number $n$ and wave vector $k$. Heinonen and Taylor[15] define an electrochemical potential $\mu+\xi i_\alpha$ that minimizes the free energy of the 2D EG subject to the constraints:

$$\sum_{n,k} f_{n,k}=N\ , \tag{1}$$

$$\sum_{n,k} i_{n,k}f_{n,k}=I\ , \tag{2}$$

where $N$ is the total number of electrons in the 2D EG, $i_{n,k}$ is the current carried by the $k$th wave-vector state in the $n$th Landau level, and $I$ is the total current through the sample. The Fermi occupation function then takes the form

$$f_{n,k}=\{\exp[\beta(\varepsilon_{n,k}-\mu-\xi i_k)]+1\}^{-1}\ , \tag{3}$$

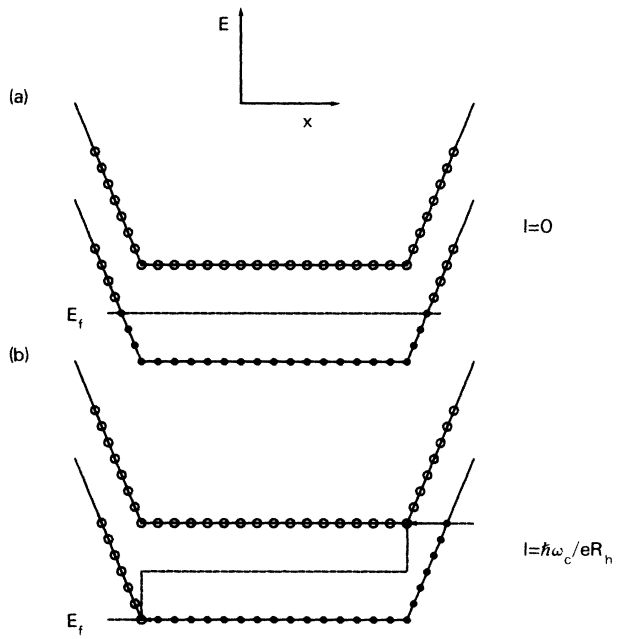


FIG. 9. Schematic energy-level diagram for our simple model for breakdown in a single channel. As current is passed through the channel, the effective chemical potential on the right side of the channel increases and the effective chemical potential on the left side decreases. If the chemical potential in the absence of an applied current is midway between Landau levels, then the left-edge states line up with the next-higher Landau level bulk states when $I=\hbar\omega_c/eR_H$. This makes interlevel scattering energetically allowed. At the same time the chemical potential at the left edge is lowered to line up with the bulk states in the filled Landau level, making intralevel scattering possible. If $\mu_0$ is higher or lower than midway between Landau levels, then the critical current for intralevel or interlevel scattering is correspondingly reduced.

where $\beta=1/k_BT$, and $k_B$ is Boltzmann's constant. As Heinonen and Taylor point out, this occupation function has the interesting property that states with higher energy are less likely to be occupied, but current-carrying states are more likely to be occupied. The current $i_{n,k}$ carried by the state $|n,k\rangle$ is given by

$$i_{n,k}=\frac{c}{BL_y}\frac{\partial\varepsilon_{n,k}}{\partial x_k} . \tag{4}$$

We need a form for the energies $\varepsilon_{n,k}$ in order to solve Eqs. (1)—(4). We assume for simplicity that the potential well that confines the electrons in the single channel threading through the constriction is such that the energy of the $k$th state in the $n$th Landau level is given by

$$\varepsilon_{n,k}=\begin{cases}(n+\frac{1}{2})\hbar\omega_c+\gamma(-L_x/2-x_k), & x_k<-L_x/2\\ (n+\frac{1}{2})\hbar\omega_c+\gamma(x_k-L_x/2), & x_k>L_x/2\\ (n+\frac{1}{2})\hbar\omega_c, & -L_x/2<x_k<L_x/2.\end{cases} \tag{5}$$

In this expression $x_k=kl_B^2$ is the center position of the harmonic-oscillator wave function, and $L_x$ is the width of the conducting channel. The parameter $\gamma$, which sets the steepness of the potential-well walls, cancels out of these calculations. If we take the low-temperature limit $\beta\rightarrow\infty$ we find that the maximum occupied current-carrying state has energy:

$$\varepsilon_{n,k}^{\max}=\mu_0\mp\frac{eIR_H}{2} , \tag{6}$$

where $\mu_0$ is the Fermi level of the 2D EG in the absence of an applied current, the positive sign is taken for states at the right edge of the constriction, and the negative sign is taken for states at the left edge of the constriction. This result has the reassuring property that the difference in chemical potential between the two edges of the conducting channel is the Hall voltage.

Figure 9 gives a schematic energy-band diagram for breakdown in a single channel with $\mu_0$ halfway between the lowest and next-higher Landau levels. As current is passed through the channel, current-carrying states on the right-hand side of the channel are filled, and states on the left-hand side of the channel are emptied. When the critical current $I_c=\hbar\omega_c/eR_H$ is exceeded filled states in the lowest Landau level on the right edge line up with the bulk states in the next higher level, making interlevel scattering energetically allowed. At the same time bulk states on the left edge are emptied, making intralevel scattering possible. If $\mu_0$ is originally above the midpoint between Landau levels, then the critical current for interlevel scattering is correspondingly reduced. If $\mu_0$ is below the midpoint between Landau levels, the critical current for intralevel scattering is reduced. This explains the roughly triangular dependence of breakdown voltages on applied field.

Even if dissipative scattering is energetically allowed, it only occurs with appreciable frequency if other factors are favorable. For example, the potential gradients at the edges of the current-carrying channels must be large enough for interband scattering to occur. Also, some source of momentum such as phonon emission must be present for intraband scattering to occur. Finally, for odd filling factors the interband scattering must involve a spin-flip process, since in that case the filled and empty bands have opposite spin.

### B. Multichannel picture

One of the striking features of our data is the structure in the breakdown characteristics at multiples of $\hbar\omega_c$ as seen in Figs. 2 and 8. There are at least two possible explanations for this sharp structure. One is that within a single channel the filled current-carrying states line up with successively higher-lying Landau bands and extra dissipation occurs. Within our simple model this would give structure at odd multiples of the cyclotron energy. However, we also observe structure at even multiples of $\hbar\omega_c$ (see Fig. 8). A second possibility would occur if there were multiple channels in parallel feeding the single channel through the constriction. We suggest that for $N$ channels in parallel, secondary structure in the current-voltage characteristic will occur at a voltage $N$ times the cyclotron energy. This can be understood as follows. The total current through a given cross section of the 2D EG is shared between the open channels. For dissipation to occur for a series of channels in parallel, they must all be dissipative, otherwise current would shunt from the dissipative to the nondissipative channels. Therefore dissipation will not occur until all of the channels have sufficient voltage drop across them to cause breakdown, at $eV_H=N\hbar\omega_c$.

There are also indications of multiple current paths completely through the constriction under certain conditions. An example is the critical Hall voltage versus filling factor curve shown in Fig. 7. An interpretation of the rapid increase in critical Hall field above about 0.135 $T^{-1}$ in this figure is that below this field there is a single conducting channel through the constriction, but as the Fermi level rises, other channels which were previously pinched off become conducting and the critical Hall voltage is correspondingly increased. As the Fermi level rises further, most of the conducting channels have partially filled next-higher Landau levels and are dissipative, so that again only one channel is involved in conduction and breakdown as the current through the channel is increased.

## V. CONCLUSIONS

In conclusion, we have shown that when a 2D EG in the quantum Hall state is laterally constricted, structure appears in the breakdown characteristics at energies corresponding to the cyclotron energies for even filling factors, or the exchange enhanced spin-spin splittings for odd filling factors. We have presented a simple model for this effect which explains in a natural way why structure appears at these energies and why the observed gaps have a roughly triangular dependence on magnetic field around

integer filling factors. Interpretation of the data in terms of this model implies that interlevel as well as intralevel scattering occurs in the dissipation process, and therefore large local potential gradients must be present in these samples. These large gradients may occur at the edges of conducting channels through the constriction. Finally, we interpret sharp structure at multiples of the cyclotron energy, and large critical currents for certain conditions of electron density and filling factor, in terms of a picture in which multiple current paths exist in the constriction region.

## ACKNOWLEDGMENTS

We would like to thank S. von Molnar, F. Fang, and G. Timp for loaning their experimental apparatus for some of our measurements. Some of the measurements were done at Francis Bitter National Magnet Laboratory (Cambridge, Massachusetts) which is supported in part by a grant by the National Science Foundation. We would like to thank Ben Parker for fabrication of some of our samples. We would also like to thank M. H. Brodsky and P. J. Stiles for suggesting the pseudo-Hall bar geometry.

## APPENDIX

In the presence of a magnetic field $\mathbf{H}=H\hat{\mathbf{z}}$ the electrostatics for the 2D EG system are defined by the fundamental constitutive equation:[13]

$$\mathbf{E}+\rho_H\mathbf{J}\times\hat{\mathbf{z}}=\sigma^{-1}\mathbf{J}\,, \tag{A1}$$

where $\mathbf{E}$ is the electric field, $\rho_H=R_HH$ is the Hall resistivity, $\sigma^{-1}$ is the Ohmic resistivity, and $\mathbf{J}$ is the current density. The Hall angle $\delta$ between the current and electric field is given by $\tan\delta=\sigma\rho_H$. Under steady-state conditions $\mathbf{E}$ can be written as the gradient of a potential $\psi$ which satisfies the two-dimensional Laplaces equation $\nabla^2\psi=0$. In Fig. 10(a) we show equipotential contour plots for a numerical solution of Laplaces equation for a $5\times1$ rectangular bar geometry with external pads, insulating boundaries, and a Hall angle given by $\tan\delta=1000$. The boundary conditions are set either by the potentials of the contacts, or are derived from Eq. (7) by the condition that no current flows through the insulating edges. The current, which follows the equipotential lines, flows from the corner of one contact to the opposite corner of the other. The edges are at equipotentials; the longitudinal resistance as measured by the voltage drops along one edge or the other are zero. In the limit of small Hall-bar width-to-length ratio the fields are completely transverse and uniform from edge to edge.

The solution to Laplace's equation for the constricted geometry can be found by using the conformal mapping

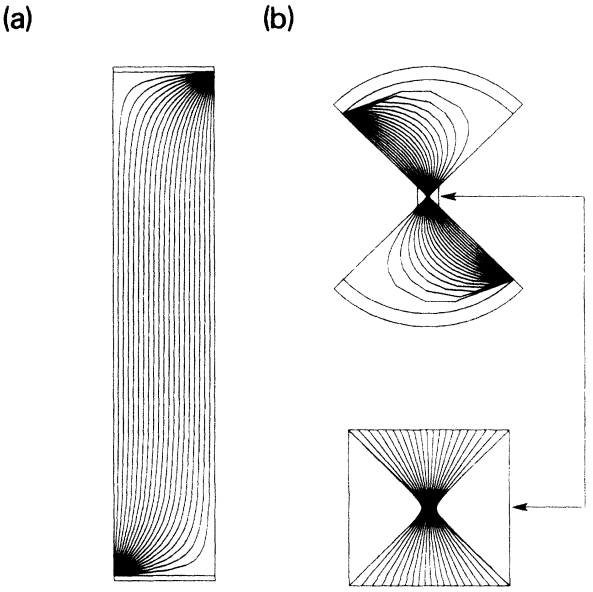


FIG. 10. Equipotential contour plots for a $5\times1$ rectangular Hall-bar geometry sample in the quantum Hall state. The conformal mapping $z=d\cosh w$ takes the Hall bar to a constriction. We argue that the constriction geometry is equivalent to a short, narrow, Hall-bar geometry when the Hall angle is close to $\pi/2$.

$z=d\cosh w$. This takes a rectangular Hall-bar sample in the complex $w=\zeta_1+i\zeta_2$ plane to a constriction in the complex $z=x+iy$ plane. Figure 10(b) shows the contour plots for the constriction geometry. The essential features of the Hall-bar geometry are retained. The edges are equipotential surfaces, so the longitudinal resistance is still zero. In the limiting case where the width of the constriction is small relative to the distance between contacts, and the Hall angle is close to $\pi/2$, and with the contact potentials at $\mp V$, the potential in the constricted region is given by

$$\psi=V+\mathrm{Re}\left[\frac{2iV}{\pi}\ln\left\{\frac{z}{d}+\left[\left[\frac{z}{d}\right]^2-1\right]^{1/2}\right\}\right]. \tag{A2}$$

In this limit the field at the edge of the constriction waist is only $\sqrt{2}$ times larger than that in the middle, and falls off with a length set by the constriction width away from the waist. Since the cyclotron orbital length $l_B$ (about 10 nm) is much smaller than the constriction width (about 1 $\mu$m), and since the edges of the sample are equipotential surfaces, it does not matter where the voltage contacts are made, and the constriction geometry is equivalent to a Hall-bar geometry.

[1]T. Ando, A. B. Fowler, and F. Stern, Rev. Mod. Phys. **54**, 437 (1982).

[2]K. von Klitzing, G. Dorda, and M. Pepper, Phys. Rev. Lett. **45**, 494 (1980).

[3]G. Ebert, K. von Klitzing, K. Ploog, and G. Weimann, J. Phys. C **16**, 5441 (1983).

[4]M. E. Cage, R. F. Dziuba, B. F. Field, E. R. Williams, S. M. Girvin, A. C. Gossard, D. C. Tsui, and R. J. Wagner, Phys. Rev. Lett. **51**, 1374 (1983).

[5]S. Komiyama, T. Takamasu, S. Hiyamizu, and S. Sasa, Solid

State Commun. **54**, 479 (1985).
[6]F. Kuckar, G. Bauer, G. Weimann, and H. Burkhard, Surf. Sci. **142**, 196 (1984).
[7]Ch. Simon, B. B. Goldberg, F. F. Fang, M. K. Thomas, and S. Wright, Phys. Rev. B **33**, 1190 (1986).
[8]L. Smrčka, J. Phys. C **18**, 2897 (1985).
[9]P. Streda, Phys. Status Solidi B **124**, K97 (1984).
[10]P. Streda and K. von Klitzing, J. Phys. C **17**, L483 (1984).
[11]O. Heinonen, P. L. Taylor, and S. M. Girvin, Phys. Rev. B **30**, 3016 (1984).
[12]H. Z. Zheng, K. K. Choi, D. C. Tsui, and G. Weimann, Phys. Rev. Lett. **55**, 1144 (1985).
[13]Th. Englert, D. C. Tsui, A. C. Gossard, and Ch. Uihlein, Surf. Sci. **113**, 215 (1982).
[14]K. von Klitzing, G. Dorda, and M. Pepper, Phys. Rev. Lett. **45**, 494 (1980).
[15]O. Heinonen and P. L. Taylor, Phys. Rev. B **32**, 633 (1985).
[16]A. H. MacDonald and P. Streda, Phys. Rev. B **29**, 1616 (1984).
[17]B. I. Halperin, Phys. Rev. B **25**, 2185 (1982).
[18]G. Ebert, K. von Klitzing, and G. Weimann, J. Phys. C **18**, L257 (1985).
[19]R. W. Rendell and S. M. Girvin, Phys. Rev. B **23**, 6610 (1981).